

Synthesis, Structure, and Ion-Binding Properties of Luminescent Gold(I) Alkynylcalix[4]crown-5 Complexes

Vivian Wing-Wah Yam,* Sung-Kong Yip, Li-Hua Yuan, Kai-Leung Cheung, Nianyong Zhu, and Kung-Kai Cheung

Open Laboratory of Chemical Biology of the Institute of Molecular Technology for Drug Discovery and Synthesis,[†] Department of Chemistry, and Centre for Carbon-Rich Molecular and Nano-Scale Metal-Based Materials Research, The University of Hong Kong, Pokfulam Road, Hong Kong SAR, People's Republic of China

Received January 13, 2003

A series of luminescent dinuclear gold(I) alkynylcalix[4]crown-5 complexes, $[(R_nR'_{3-n}P)Au]_2L$ ($n = 0-3$) ($R = Ph$, $R' = o-Tol$, $p-Tol$) ($H_2L = 5,17$ -diethynyl-25,27-dimethoxycalix[4]arene-crown-5, have been synthesized and structurally characterized. The binding properties of the complexes toward alkali metal ions (K^+ and Na^+) have been studied by UV-visible spectrophotometry. The dinuclear gold(I) alkynylcalix[4]crown-5 complexes were shown to exhibit preferential binding toward K^+ over Na^+ ions.

Introduction

Ion recognition plays important roles in biology and chemistry, as well as in biomedical and environmental science. In biological systems, metal ions such as sodium, potassium, calcium, and magnesium ions are involved in nerve impulse transmission, muscle contraction, and cell activity regulation. Lithium ion has also been used for patients under depression treatment. With regard to environmental and ecological issues, heavy metal ions such as lead, cadmium, and radioactive metal ions have attracted enormous attention and worldwide concern. Thus, the ability to detect or recognize specific metal ions can be invaluable.

During the past decade, there has been a growing interest in the development of calixarenes as ion receptors.¹ Calixarenes have proved themselves as important building blocks in supramolecular chemistry owing to their unique molecular structures, simple one-pot preparations, possible modifications of the lower and upper rims, and their "tunable" molecular shapes and conformations.²⁻⁴ Another related class of compounds that has also received considerable attention as ion receptor molecules in recent years is the calixcrown,⁵ in which the lower rim of the calixarene is linked by bridging polyethyleneoxy moieties. High affinities for complexation of alkali and alkaline-earth metal ions have been reported for calixcrowns.⁶ The majority of the work in this area has mainly been focused on the use of an

organic system as luminophore,⁷ with metal-based luminophores being relatively less extensively explored.⁸ Recently, we reported the synthesis of a dinuclear gold(I) alkynyl complex of calixcrown and have demonstrated its selective ion-binding properties toward alkali metal ions.⁹ As an extension of this work, a series of related complexes with various phosphine ligands have been designed and synthesized. It is hoped that through a systematic variation of the electronic and steric effects of the aryl group on the phosphine ligands, the ion-binding properties of the complexes can be tuned. Herein are reported the synthesis, electronic absorption, luminescence, and ion-binding properties of a series of dinuclear gold(I) alkynylcalix[4]crown-5 complexes. The X-ray crystal structures of all the complexes have been determined by X-ray crystallography.

Experimental Section

Materials and Reagents. Potassium fluoride and tetraethylene glycol-di-*p*-toluenesulfonate were purchased from Aldrich Chemical Co. (Trimethylsilyl)acetylene, copper(I) iodide, and triethylamine were purchased from Lancaster Synthesis Ltd. Cesium carbonate was purchased from Strem Chemical Inc. Dichlorobis(triphenylphosphine)palladium(II)¹⁰ and 5,17-diiodo-25,27-dimethoxycalix[4]arene¹¹ were prepared according to the literature procedures. All the $[(R_nR'_{3-n}P)AuCl]$ precursor complexes were synthesized by modification of the literature methods.¹² Tetra-*n*-butylammonium hexafluorophos-

* Corresponding author. Tel: (852) 2859-2153. Fax: (852) 2857-1586. E-mail: wwyam@hku.hk.

[†] Area of Excellence Scheme, University Grants Committee (Hong Kong).

(1) Valeur, B.; Leray, I. *Coord. Chem. Rev.* **2000**, *205*, 3.

(2) (a) Gutsche, C. D. *Calixarenes: Monographs in Supramolecular Chemistry*; The Royal Society of Chemistry: Cambridge, 1989. (b) Gutsche, C. D. *Calixarenes Revisited*; The Royal Society of Chemistry: Cambridge, 1998. (c) Asfari, Z. *Calixarenes 2001*; Kluwer Academic Publishers: Dordrecht, 2001.

(3) Gutsche, C. D.; Iqbal, M. *Org. Synth., Coll. Vol.* **1993**, *8*, 75.

(4) (a) Shinkai, S. *Tetrahedron* **1993**, *49*, 8933. (b) Böhrer, V. *Angew. Chem., Int. Ed. Engl.* **1995**, *34*, 713.

(5) Stephane, P. R.; Frederic, C.; Laurence, N.; Marc, L. *J. Chem. Soc., Perkin Trans.* **2001**, *2*, 1426.

(6) Alfieri, C.; Dradi, E.; Pochini, A.; Ungaro, R.; Andreotti, G. D. *J. Chem. Soc., Chem. Commun.* **1983**, 1075.

(7) (a) Shinkai, S.; Matsumoto, H. *Chem. Lett.* **1994**, 2431. (b) Kubo, Y.; Maeda, S.; Tokita, S.; Kubo, M. *Nature* **1996**, *382*, 522. (c) Ji, H. F.; Dabestani, R.; Brown, G. M.; Sachleben, R. A. *Chem. Commun.* **2000**, 833.

(8) Xu, W.; Rourke, J. P.; Vittal, J. J.; Puddephatt, R. J. *J. Chem. Soc., Chem. Commun.* **1993**, 2, 145.

(9) Yam, V. W. W.; Cheung, K. L.; Yuan, L. H.; Wong, K. M. C.; Cheung, K. K. *Chem. Commun.* **2000**, 16, 1513.

(10) Chatt, J.; Mann, F. G. *J. Chem. Soc.* **1939**, 1622.

(11) Klenke, B.; Friedrichsen, W. *J. Chem. Soc., Perkin Trans. 1* **1998**, *20*, 3377.

(12) Bruce, M. I.; Nicholson, B. K.; Shawkataly, O. B. *Inorg. Synth.* **1989**, *26*, 324.

phate was recrystallized twice from hot absolute ethanol and then dried under vacuum for 12 h before use. Dichloromethane (Lab Scan, AR) was purified and distilled using standard procedures before use. All other reagents were of analytical grade and were used as received. All reactions were carried out under an inert atmosphere of nitrogen using standard Schlenk techniques.

5,17-Bis(trimethylsilylethynyl)-25,27-dimethoxycalix[4]arene (Calix-TMS). Into a 250 mL two-necked round-bottomed flask was added 5,17-diiodo-25,27-dimethoxycalix[4]arene (1.00 g, 1.42 mmol), followed by a mixture of tetrahydrofuran (130 mL) and triethylamine (20 mL). After stirring for 5 min, trimethylsilylacetylene (0.56 g, 5.68 mmol), copper(I) iodide (22 mg, 0.11 mmol), and dichlorobis(triphenylphosphine)palladium(II) (80 mg, 0.11 mmol) were added to the flask under a nitrogen atmosphere. The mixture was stirred for 24 h at 42 °C. The mixture was filtered, and the filtrate was evaporated to dryness. The brown residue was purified by column chromatography on silica gel using petroleum ether/dichloromethane (1:1 v/v) as eluent to afford the product as a yellow solid. Yield: 0.486 g, 53%. ¹H NMR (300 MHz, CDCl₃, 298 K, relative to Me₄Si): δ 0.15 (s, 18H, Si-(CH₃)₃), 3.31 (d, 4H, *J* = 13.2 Hz, Ar-CH₂-Ar), 3.88 (s, 6H, OCH₃), 4.15 (d, 4H, *J* = 13.2 Hz, Ar-CH₂-Ar), 6.72–7.14 (m, 10H, Ar), 8.03 (s, 2H, OH). ¹³C NMR (125 MHz, CDCl₃, 298 K, relative to Me₄Si): δ 30.8, 63.7, 91.7, 105.9, 113.3, 125.3, 128.0, 129.3, 132.0, 132.5, 153.0, 154.0. IR (KBr disk, ν/cm⁻¹): 2905 (s), 2957 (s), ν(C-H_{aliphatic}); 2150 (m), ν(C≡C). Positive FAB-MS: *m/z* 645 [M]⁺. Anal. Found: C 73.73, H 7.16. Calcd for C₄₀H₄₄O₄Si₂·1/2H₂O: C 73.47, H 6.94.

5,17-Bis(trimethylsilylethynyl)-25,27-dimethoxycalix[4]crown-5 (CalixCr-TMS). An excess of cesium carbonate (0.40 g, 1.24 mmol) and tetraethylene glycol-di-*p*-toluene-sulfonate (0.17 g, 0.34 mmol) were added to Calix-TMS (0.20 g, 0.31 mmol) in 80 mL of acetonitrile under nitrogen atmosphere. The reaction mixture was refluxed for 24 h. The solvent was then removed under reduced pressure, and the residue was extracted with dichloromethane and washed with water. Evaporation of the dichloromethane extract yielded a yellow residue, which was triturated in diethyl ether to afford the product as a white solid. Yield: 0.212 g, 87%. ¹H NMR (300 MHz, CDCl₃, 298 K, relative to Me₄Si): δ 0.14 (s, 18H, Si-(CH₃)₃), 3.16 (d, 4H, *J* = 12.4 Hz, Ar-CH₂-Ar), 3.55–3.90 (m, 16H, OCH₂CH₂O), 4.10 (s, 6H, OCH₃), 4.37 (d, 4H, *J* = 12.4 Hz, Ar-CH₂-Ar), 6.79 (s, 4H, aryl protons *ortho* to C≡C), 6.89 (t, 2H, *J* = 7.3 Hz, aryl protons *para* to OCH₃), 7.09 (d, 4H, *J* = 7.3 Hz, aryl protons *meta* to OCH₃). ¹³C NMR (125 MHz, CDCl₃, 298 K, relative to Me₄Si): δ 31.1, 61.1, 65.8, 70.7, 70.8, 71.4, 123.0, 124.5, 128.7, 132.1, 133.5, 135.6, 156.4, 158.9. IR (KBr disk, ν/cm⁻¹): 2922 (s), 2903 (s), 2872 (s), ν(C-H_{aliphatic}); 2154 (m), ν(C≡C). Positive FAB-MS: *m/z* 803 [M]⁺, 826 [M + Na]⁺. Anal. Found: C 71.63, H 7.05. Calcd for C₄₈H₅₈O₇Si₂: C 71.78, H 7.28.

5,17-Diethynyl-25,27-dimethoxycalix[4]arene-crown-5 (H₂L). Potassium fluoride (0.12 g, 2.05 mmol) was added to CalixCr-TMS (0.10 g, 0.13 mmol) in dimethylformamide. The mixture was stirred under nitrogen in an oil bath at 65 °C for 3 h. The reaction was quenched with dilute hydrochloric acid, and the product was extracted with chloroform and washed with water. After removing the solvent, the residue was triturated in diethyl ether to afford a pale brown solid. Yield: 64 mg, 75%. ¹H NMR (300 MHz, CDCl₃, 298 K, relative to Me₄Si): δ 2.77 (s, 2H, C≡CH), 3.16 (d, 4H, *J* = 12.6 Hz, Ar-CH₂-Ar), 3.56–3.93 (m, 16H, OCH₂CH₂O), 4.10 (s, 6H, OCH₃), 4.38 (d, 4H, *J* = 12.6 Hz, Ar-CH₂-Ar), 6.76 (s, 4H, aryl protons *ortho* to C≡C), 6.88 (t, 2H, *J* = 7.3 Hz, aryl protons *para* to OCH₃), 7.08 (d, 4H, *J* = 7.3 Hz, aryl protons *meta* to OCH₃). ¹³C NMR (125 MHz, CDCl₃, 298 K, relative to Me₄Si): δ 31.1, 61.2, 70.8, 70.9, 71.5, 73.4, 75.4, 84.3, 115.9, 123.1, 128.7, 132.1, 133.8, 156.4, 158.9. IR (KBr disk, ν/cm⁻¹): 3292 (s), ν(C-H_{alkynyl}); 2909 (s), 2868 (s), ν(C-H_{aliphatic}); 2107 (w), ν(C≡C).

Positive FAB-MS: *m/z* 658 [M]⁺, 681 [M + Na]⁺. Anal. Found: C 72.86, H 6.24. Calcd for C₄₂H₄₂O₇·1/2CH₂Cl₂: C 72.79, H 6.18.

[(PPh₃)Au]₂L (1). To a stirred solution of H₂L (30 mg, 0.046 mmol) in tetrahydrofuran (15 mL) was added an excess of sodium ethoxide (freshly prepared from sodium (10 mg, 0.43 mmol) in ethanol (15 mL)) and chloro(triphenylphosphine)gold(I) (47 mg, 0.095 mmol). The reaction mixture was then stirred under an inert atmosphere of nitrogen for 4 h. The solution was extracted with dichloromethane and washed with water. Subsequent recrystallization by layering *n*-hexane into the concentrated dichloromethane solution of the product gave **1** as pale yellow crystals. Yield: 54 mg, 75%. ¹H NMR (300 MHz, CDCl₃, 298 K, relative to Me₄Si): δ 3.12 (d, 4H, *J* = 12.6 Hz, Ar-CH₂-Ar), 3.65–4.00 (m, 16H, OCH₂CH₂O), 4.05 (s, 6H, OCH₃), 4.32 (d, 4H, *J* = 12.6 Hz, Ar-CH₂-Ar), 6.55–7.10 (m, 10H, Ar), 7.25–7.58 (m, 30H, PPh₃). ³¹P NMR (202 MHz, CDCl₃, 298 K, relative to 85% H₃PO₄): δ 43.5 (s, PPh₃). IR (KBr disk, ν/cm⁻¹): 2918 (s), 2866 (s), ν(C-H_{aliphatic}); 2099 (w), ν(C≡C). Positive FAB-MS: *m/z* 1597 [M + Na]⁺. Anal. Found: C 59.54, H 4.72. Calcd for C₇₈H₇₀O₇Au₂P₂: C 59.47, H 4.48.

[(PPh₂(*p*-Tol)Au]₂L (2). This complex was prepared similarly to **1** except chloro(diphenyl-*p*-tolylphosphine)gold(I) (46 mg, 0.088 mmol) was used instead of chloro(triphenylphosphine)gold(I). The product was recrystallized from dichloromethane/*n*-hexane to give **2** as pale yellow crystals. Yield: 52 mg, 71%. ¹H NMR (300 MHz, CDCl₃, 298 K, relative to Me₄Si): δ 2.34 (s, 6H, PC₆H₄CH₃), 3.14 (d, 4H, *J* = 12.2 Hz, Ar-CH₂-Ar), 3.67–4.01 (m, 16H, OCH₂CH₂O), 4.04 (s, 6H, OCH₃), 4.33 (d, 4H, *J* = 12.2 Hz, Ar-CH₂-Ar), 6.42–7.06 (m, 10H, Ar), 7.21–7.52 (m, 28H, PPh₂Tol). ³¹P NMR (202 MHz, CDCl₃, 298 K, relative to 85% H₃PO₄): δ 42.16 (s, PPh₂Tol). IR (KBr disk, ν/cm⁻¹): 2855 (s), 2920 (s), ν(C-H_{aliphatic}); 2087 (w), ν(C≡C). Positive FAB-MS: *m/z* 1626 [M + Na]⁺, 1642 [M + K]⁺. Anal. Found: C 59.18, H 4.80. Calcd for C₈₀H₇₄O₇Au₂P₂·1/2CH₂Cl₂·1/2C₆H₁₄: C 59.38, H 4.89.

[(PPh(*p*-Tol)₂)]Au₂L (3). This complex was prepared similarly to **1** except chloro(phenyldi-*p*-tolylphosphine)gold(I) (48 mg, 0.092 mmol) was used instead of chloro(triphenylphosphine)gold(I). The product was recrystallized from dichloromethane/*n*-hexane to give **3** as pale yellow crystals. Yield: 56 mg, 74%. ¹H NMR (300 MHz, CDCl₃, 298 K, relative to Me₄Si): δ 2.32 (s, 12H, PC₆H₄CH₃), 3.12 (d, 4H, *J* = 12.5 Hz, Ar-CH₂-Ar), 3.66–4.00 (m, 16H, OCH₂CH₂O), 4.05 (s, 6H, OCH₃), 4.31 (d, 4H, *J* = 12.5 Hz, Ar-CH₂-Ar), 6.56–7.06 (m, 10H, Ar), 7.16–7.49 (m, 26H, PPh₂Tol₂). ³¹P NMR (202 MHz, CDCl₃, 298 K, relative to 85% H₃PO₄): δ 41.16 (s, PPh₂Tol₂). IR (KBr disk, ν/cm⁻¹): 2864 (s), 2920 (s), ν(C-H_{aliphatic}); 2103 (w), ν(C≡C). Positive FAB-MS: *m/z* 1654 [M + Na]⁺, 1670 [M + K]⁺. Anal. Found: C 59.65, H 4.80. Calcd for C₈₂H₇₈O₇Au₂P₂·1/2CH₂Cl₂·1/2C₆H₁₄: C 59.81, H 5.05.

[(P(*p*-Tol)₃)]Au₂L (4). This complex was prepared similarly to **1** except chloro(tri-*p*-tolylphosphine)gold(I) (49 mg, 0.091 mmol) was used instead of chloro(triphenylphosphine)gold(I). The product was recrystallized from acetone/*n*-hexane to give **4** as pale yellow crystals. Yield: 48 mg, 67%. ¹H NMR (300 MHz, CDCl₃, 298 K, relative to Me₄Si): δ 2.31 (s, 18H, PC₆H₄CH₃), 3.12 (d, 4H, *J* = 12.9 Hz, Ar-CH₂-Ar), 3.67–4.01 (m, 16H, OCH₂CH₂O), 4.08 (s, 6H, OCH₃), 4.31 (d, 4H, *J* = 12.9 Hz, Ar-CH₂-Ar), 6.49–7.09 (m, 10H, Ar), 7.15–7.44 (m, 24H, PTol₃). ³¹P NMR (202 MHz, CDCl₃, 298 K, relative to 85% H₃PO₄): δ 40.79 (s, PTol₃). IR (KBr disk, ν/cm⁻¹): 2834 (s), 2915 (s), ν(C-H_{aliphatic}); 2021 (w), ν(C≡C). Positive FAB-MS: *m/z* 1660 [M + H]⁺, 1682 [M + Na]⁺. Anal. Found: C, 59.69, H, 5.03. Calcd for C₈₄H₈₂O₇Au₂P₂·CH₃COCH₃·2H₂O: C, 59.59, H, 5.29.

[(P(*o*-Tol)₃)]Au₂L (5). This complex was prepared similarly to **1** except chloro(tri-*o*-tolylphosphine)gold(I) (49 mg, 0.091 mmol) was used instead of chloro(triphenylphosphine)gold(I). The product was recrystallized from dichloromethane/*n*-hexane

to give **5** as pale yellow crystals. Yield: 50 mg, 70%. ^1H NMR (300 MHz, CDCl_3 , 298 K, relative to Me_4Si): δ 2.66 (s, 18H, $\text{PC}_6\text{H}_4\text{CH}_3$), 3.09 (d, 4H, $J = 11.8$ Hz, $\text{Ar}-\text{CH}_2-\text{Ar}$), 3.63–3.93 (m, 16H, $\text{OCH}_2\text{CH}_2\text{O}$), 3.99 (s, 6H, OCH_3), 4.29 (d, 4H, $J = 11.8$ Hz, $\text{Ar}-\text{CH}_2-\text{Ar}$), 6.56–7.39 (m, 34H, Ar, PTol_3). ^{31}P NMR (202 MHz, CDCl_3 , 298 K, relative to 85% H_3PO_4): δ 24.63 (s, PTol_3). IR (KBr disk, ν/cm^{-1}): 2840 (s), 2913 (s), $\nu(\text{C}-\text{H}_{\text{aliphatic}})$; 2018 (w), $\nu(\text{C}\equiv\text{C})$. Positive FAB-MS: m/z 1660 $[\text{M} + \text{H}]^+$, 1682 $[\text{M} + \text{Na}]^+$, 1698 $[\text{M} + \text{K}]^+$. Anal. Found: C 57.71, H 4.94. Calcd for $\text{C}_{84}\text{H}_{82}\text{O}_7\text{Au}_2\text{P}_2\cdot\text{CH}_2\text{Cl}_2\cdot\text{H}_2\text{O}$: C 57.93, H 4.92.

Physical Measurements and Instrumentation. UV/VIS spectra were obtained on a Hewlett-Packard 8452A diode array spectrophotometer, IR spectra as KBr disks on a Bio-Rad FTS-7 Fourier transform infrared spectrophotometer (4000–400 cm^{-1}), and steady-state excitation and emission spectra on a Spex Fluorolog 111 fluorescence spectrophotometer. Solid-state photophysical studies were carried out with solid sample contained in a quartz tube inside a quartz-walled Dewar flask. Solid-state samples at 77 K were conducted with liquid nitrogen in the optical Dewar flask. Excited-state lifetimes of solution samples were measured using a conventional laser system. The excitation source was the 355 nm output (third harmonic, 8 ns) of a Spectra-Physics Quanta-Ray Q-switched GCR-150 pulsed Nd:YAG laser (10 Hz). Luminescence quantum yield was measured by the optical dilute method reported by Demas and Crosby.¹³ The luminescence quantum yield of the sample was determined according to eq 1:

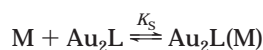
$$\phi_s = \phi_r(B_r/B_s)(n_s/n_r)^2(D_s/D_r) \quad (1)$$

where the subscripts s and r refer to the sample and reference solutions, respectively, $B = 1 - 10^{-A}$. A is the absorbance at the excitation wavelength, L is the path length, n is the refractive index of the solvent, and D is the integrated emission intensity. A degassed aqueous solution of quinine sulfate in 1.0 N H_2SO_4 solution ($\phi_{\text{em}} = 0.546$, excitation wavelength at 365 nm) was used as the reference.¹³

All solutions for photophysical studies were degassed on a high-vacuum line in a two-compartment cell consisting of a 10 mL Pyrex bulb and a 1 cm path length quartz cuvette and sealed from the atmosphere by a Bibby RotaFlo HP6 Teflon stopper. The solutions were subject to not less than four freeze–pump–thaw cycles.

^1H NMR spectra were recorded on a Bruker DPX-300 FT-NMR spectrometer (300 MHz) in CDCl_3 at 298 K, and chemical shifts are reported relative to Me_4Si . ^{31}P and ^{13}C NMR spectra were recorded on a Bruker DRX-500 FT-NMR spectrometer (202 MHz for ^{31}P and 125 MHz for ^{13}C) in CDCl_3 at 298 K, and chemical shifts are reported relative to 85% H_3PO_4 and Me_4Si , respectively. Positive FAB mass spectra were recorded on a Finnigan MAT95 mass spectrometer. Elemental analyses of the new complexes were performed on a Carlo Erba 1106 elemental analyzer at the Institute of Chemistry, Chinese Academy of Sciences.

The electronic absorption spectral titration for binding constant determination was performed with a Hewlett-Packard 8452A diode array spectrophotometer at 25 $^\circ\text{C}$, which was controlled by a Lauda RM6 compact low-temperature thermostat. Supporting electrolyte (0.1 mol dm^{-3} $n\text{Bu}_4\text{NPF}_6$) was added to maintain a constant ionic strength of the sample solution in order to avoid any changes arising from a change in the ionic strength of the medium. The binding constants, K_s , for the 1:1 complexation that control the equilibrium between an alkali cation M, the dinuclear gold(I) alkynylcalix-[4]crown complex Au_2L , and their adduct $\text{Au}_2\text{L}(\text{M})$,



(13) Demas, J. N.; Crosby, G. A. *J. Phys. Chem.* **1971**, *75*, 991.

where K_s can be written as

$$K_s = \frac{[\text{Au}_2\text{L}(\text{M})]}{[\text{Au}_2\text{L}][\text{M}]}$$

were obtained by a nonlinear least-squares fit of the absorbance (X) versus the concentration of the metal ion added (C_m) according to eq 2:¹⁴

$$X = X_0 + \frac{X_{\text{lim}} - X_0}{2C_0} [C_0 + C_m + 1/K_s - [(C_0 + C_m + 1/K_s)^2 - 4C_0C_m]^{1/2}] \quad (2)$$

where C_0 is the initial concentration of the gold(I) complexes, and X_0 , X , and X_{lim} are the initial absorbance of the gold(I) complexes, the absorbance after the addition of a given amount of salt at concentration C_m , and the limiting absorbance of the gold(I) complexes in the fully complexed state, respectively, at a selected wavelength.

Crystal Structure Determination. Single crystals of **1** were obtained by layering n -hexane into a dichloromethane solution of the complex, the crystal structure of which has been communicated previously.⁹

Single crystals of **2**, **3**, and **5** were obtained by layering n -hexane into a dichloromethane solution of the respective complex. Single crystals of **4** were obtained by layering n -hexane into an acetone solution of the complex. All the experimental details are given in Table 1. The crystals of **2–5** of dimensions $0.3 \times 0.3 \times 0.1$ mm, $0.60 \times 0.20 \times 0.05$ mm, $0.4 \times 0.25 \times 0.2$ mm, and $0.3 \times 0.25 \times 0.15$ mm, respectively, mounted in a glass capillary were used for data collection at 28 $^\circ\text{C}$ on a MAR diffractometer. The images were interpreted and intensities integrated using the program DENZO.¹⁵ The structures were solved by direct methods employing the SHELXS-97 program¹⁶ on a PC. The positions of H atoms of all complexes were calculated based on riding mode with thermal parameters equal to 1.2 times that of the associated C atoms and participated in the calculation of final R -indices.¹⁷

For complex **2**, one crystallographic asymmetric unit consisted of one formula unit, inclusive of one CH_2Cl_2 and one n -hexane solvent molecules. In the final stage of least-squares refinement, most non-hydrogen atoms were refined anisotropically, except the C atoms of n -hexane, which were refined isotropically. H atoms (except those on n -hexane) were generated by the program SHELXL-97.¹⁸ One phosphine ligand was found to be the normal PPh_2Tol , but the other one had the methyl group disordered on two phenyl rings. One hexagon-ring of C(26) to C(31) is restrained to be a normal hexagonal ring (C–C distance 1.39 Å and C–C–C angle 120 $^\circ$). The n -hexane molecule was disordered and was set at two positions. For convergence of least-squares refinements, the C–C bond lengths of the hexane chain were restrained to be similar.

(14) Bourson, J.; Pouget, J.; Valeur, B. *J. Phys. Chem.* **1993**, *97*, 4552.

(15) Otwinowski, Z.; Minor, W. Processing of X-ray Diffraction Data Collected in Oscillation Mode. *Methods in Enzymology*, Volume 276: Macromolecular Crystallography; Carter C. W., Sweet, R. M., Jr., Eds.; Academic Press: New York, 1997; Part A, pp 307–326.

(16) Sheldrick, G. M. *SHELX97*, Programs for Crystal Structure Analysis (Release 97-2); University of Goettingen: Germany, 1997.

(17) Since the structure refinements are against F^2 , R -indices based on F^2 are larger than (more than double) those based on F . For comparison with older refinements based on F and an OMIT threshold, a conventional index R_1 based on observed F values larger than $4\sigma(F_o)$ is also given (corresponding to intensity $\geq 2\sigma(I)$). $wR_2 = \{\sum[w(F_o^2 - F_c^2)^2]/\sum[w(F_o^2)^2]\}^{1/2}$, $R_1 = \sum||F_o| - |F_c||/\sum|F_o|$, the goodness of fit is always based on F^2 : $\text{GooF} = S = \{\sum[w(F_o^2 - F_c^2)^2]/(n - p)\}^{1/2}$, where n is the number of reflections and p is the total number of parameters refined. The weighting scheme is $w = 1/[\sigma^2(F_o^2) + (aP)^2 + bP]$, where P is $[2F_c^2 + \text{Max}(F_o^2, 0)]/3$.

(18) Sheldrick, G. M. *SHELX97*, Programs for Crystal Structure Analysis (Release 97-2); University of Goettingen: Germany, 1997.

Table 1. Crystal and Structure Determination Data for 1–5

	1	2	3	4	5
empirical formula	[C ₇₈ H ₇₂ Au ₂ O ₈ P ₂]	[C ₈₇ H ₈₉ Au ₂ Cl ₂ O ₇ P ₂]	[C ₈₉ H ₉₃ Au ₂ Cl ₂ O ₇ P ₂]	[C ₈₇ H ₈₈ Au ₂ O ₈ P ₂]	[C ₈₈ H ₈₆ Au ₂ Cl ₈ O ₇ P ₂]
fw	1593.30	1773.36	1801.41	1717.45	1995.04
cryst size (mm)	0.25 × 0.2 × 0.1	0.3 × 0.3 × 0.1	0.6 × 0.2 × 0.05	0.4 × 0.25 × 0.2	0.3 × 0.25 × 0.15
cryst syst	triclinic	monoclinic	monoclinic	triclinic	monoclinic
space group	<i>P</i> $\bar{1}$	<i>P</i> 2 ₁ / <i>c</i>	<i>P</i> 2 ₁ / <i>c</i>	<i>P</i> $\bar{1}$	<i>C</i> 2/ <i>c</i>
<i>a</i> (Å)	13.108(2)	22.277(4)	22.033(4)	14.828(3)	42.499(9)
<i>b</i> (Å)	15.195(2)	13.109(2)	13.257(3)	16.138(3)	21.013(4)
<i>c</i> (Å)	21.461(3)	27.775(5)	28.870(5)	16.669(3)	20.487(4)
α (deg)	83.57(2)	90	90	88.42(3)	90
β (deg)	76.71(2)	98.41(4)	98.33(2)	86.27(3)	109.44(3)
γ (deg)	65.43(2)	90	90	82.76(3)	90
<i>V</i> (Å ³)	3782(1)	8024(2)	8344(3)	3947.9(13)	17253(6)
<i>Z</i>	2	4	4	2	8
<i>F</i> (000)	1584	3556	3620	1724	7952
μ (mm ⁻¹)	3.980	3.812	3.667	3.806	3.735
density calcd (g cm ⁻³)	1.399	1.468	1.434	1.445	1.536
temperature (K)	301	301	301	301	301
wavelength (Å)	0.71073	0.71073	0.71073	0.71073	0.71069
collection range	$2\theta_{\max} = 51^\circ$ <i>h</i> : 0 to 15 <i>k</i> : -16 to 18 <i>l</i> : -25 to 25	$2\theta_{\max} = 50.94^\circ$ <i>h</i> : -21 to 26 <i>k</i> : -15 to 14 <i>l</i> : -28 to 29	$2\theta_{\max} = 51.02^\circ$ <i>h</i> : -26 to 26 <i>k</i> : -14 to 14 <i>l</i> : -32 to 33	$2\theta_{\max} = 51.04^\circ$ <i>h</i> : -16 to 16, <i>k</i> : -19 to 19 <i>l</i> : -20 to 20	$2\theta_{\max} = 50.98^\circ$ <i>h</i> : -51 to 51, <i>k</i> : -23 to 24 <i>l</i> : -24 to 24
no. of reflns collected	55 002	23 241	38 787	28 728	50 528
no. of indep reflns	12 114 [<i>R</i> (int) = 0.045]	10 048 [<i>R</i> (int) = 0.0558]	11 945 [<i>R</i> (int) = 0.0555]	13 190 [<i>R</i> (int) = 0.0290]	13 760 [<i>R</i> (int) = 0.0528]
refinement method	full-matrix least-squares on <i>F</i> ²	full-matrix least-squares on <i>F</i> ²	full-matrix least-squares on <i>F</i> ²	full-matrix least-squares on <i>F</i> ²	full-matrix least-squares on <i>F</i> ²
data/params	12 114/806	10 048/879	11 945/821	13 190/892	13 760/990
goodness-of-fit on <i>F</i> ²	2.16	0.954	0.962	1.031	0.920
final <i>R</i> indices	<i>R</i> ₁ = 0.055, ^a <i>wR</i> ₂ = 0.081 ^a	<i>R</i> ₁ = 0.0513, ^b <i>wR</i> ₂ = 0.1312 ^b	<i>R</i> ₁ = 0.0524, ^b <i>wR</i> ₂ = 0.1505 ^b	<i>R</i> ₁ = 0.0329, ^b <i>wR</i> ₂ = 0.0874 ^b	<i>R</i> ₁ = 0.0381, ^b <i>wR</i> ₂ = 0.0983 ^b
largest diff. peak and hole (e Å ⁻³)	1.15, -1.79	0.925, -0.976	1.444, -1.182	0.717, -1.272	0.835, -0.737

^a [*I* > 3 σ (*I*)]. ^b [*I* > 2 σ (*I*)].

For complex **3**, one crystallographic asymmetric unit consisted of one formula unit, one CH₂Cl₂ and one *n*-hexane solvent molecule. In the final stage of least-squares refinement, most non-hydrogen atoms were refined anisotropically, except one disordered methyl C atom attached to the phenyl ring of PR₃ and the C atoms of *n*-hexane, which were refined isotropically. H atoms (except those on *n*-hexane) were generated by the program SHELXL-97.¹⁸ The phenyl rings on PR₃ groups were restrained to normal phenyl rings. One phosphine ligand was found to be the normal PTol₂Ph, but the other one has the two methyl groups disordered on three phenyl rings. The *n*-hexane molecule was located with restraints of the C–C bond lengths to 1.55 Å.

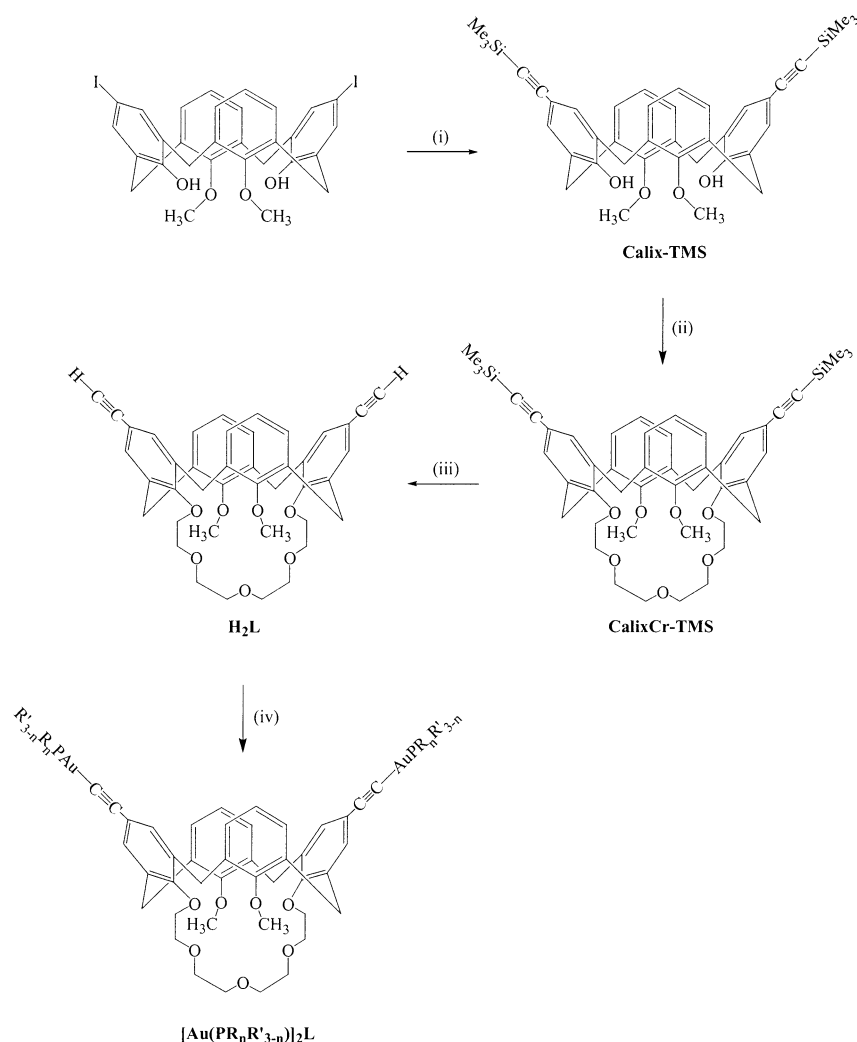
For complex **4**, the acentric space group *P*1 was chosen temporarily. Four Au atoms were located according to the direct methods. The space group was then transformed to centric *P* $\bar{1}$ and the coordinates were also transformed, so that the two Au atoms were located with the centric space group. The positions of the other non-hydrogen atoms were found after successful refinement by full-matrix least-squares using the program SHELXL-97¹⁸ on a PC. One acetone solvent molecule was also positioned. One crystallographic asymmetric unit consisted of one formula unit, inclusive of one acetone solvent molecule. In the final stage of least-squares refinement, all non-hydrogen atoms were refined anisotropically. H atoms were generated by the program SHELXL-97.¹⁸

For complex **5**, one crystallographic asymmetric unit consisted of one formula unit. In the final stage of least-squares refinement, all non-H atoms were refined anisotropically. H atoms were generated by the program SHELXL-97.¹⁸ Four dichloromethane solvent molecules were also located, in which two of them were disordered. Disordered dichloromethane molecules were restrained to have similar C–Cl and Cl–Cl distances, respectively.

Results and Discussion

Synthesis. The synthetic route for the gold(I) alkynyl-calix[4]crown-5 complexes is summarized in Scheme 1. Reaction of 5,17-diiodo-25,27-dimethoxycalix[4]arene⁷ with (trimethylsilyl)acetylene in the presence of copper(I) iodide, dichlorobis(triphenylphosphine)palladium(II), and triethylamine for 24 h at ca. 42 °C gave Calix-TMS. Subsequent reaction with tetraethylene glycol di-*p*-toluenesulfonate in the presence of cesium carbonate in acetonitrile introduces the polyether linkage at the lower rim followed by deprotection of the trimethylsilyl groups with potassium fluoride gave H₂L in moderate yield. Reaction of (R_{*n*}R'_{3-*n*}P)AuCl (*n* = 0–3) (R = Ph, R' = *o*-Tol, *p*-Tol) with H₂L in the presence of sodium ethoxide in ethanol afforded the desired complexes, [(R_{*n*}R'_{3-*n*}P)Au]₂L, as pale yellow crystals after subsequent recrystallization using dichloromethane/*n*-hexane or acetone/*n*-hexane. The identities of complexes **1–5** have been confirmed by satisfactory elemental analyses, ¹H NMR, ³¹P NMR, IR, and FAB-mass spectrometry. The structures of **1–5** have also been determined by X-ray crystallography.

Crystal Structure Determination. The perspective drawings of selected complexes **3** and **4** are shown in Figures 1 and 2, respectively. Selected bond distances and angles of complexes **1–5** are tabulated in Table 2. The coordination geometry of the two gold atoms are essentially linear, with P–Au–C bond angles showing a slight deviation from the ideal 180°, probably as a result of the steric demand of the ligands and crystal packing forces (**1**, 170.5(4)° and 177.9(4)°; **2**, 176.0(4)° and 176.6(3)°; **3**, 174.7(3)° and 176.6(3)°; **4**, 173.09(16)°

Scheme 1. Synthetic Route of Complexes 1–5^a

^a Reagents and conditions: (i) $\text{HC}\equiv\text{CSiMe}_3$, Et_3N , $\text{Pd}(\text{PPh}_3)_2\text{Cl}_2$, CuI ; (ii) tetraethylene glycol di-*p*-toluenesulfonate, Cs_2CO_3 , CH_3CN ; (iii) KF , DMF , 65°C ; (iv) NaOEt , $(\text{R}_n\text{R}'_{3-n}\text{P})\text{AuCl}$ ($n = 0-3$), EtOH/THF . ($\text{R} = \text{Ph}$, $\text{R}' = o\text{-Tol}$, $p\text{-Tol}$).

and $176.12(18)^\circ$; **5**, $175.8(2)^\circ$ and $177.1(3)^\circ$). The $\text{C}\equiv\text{C}$ bond lengths of all the complexes are typical of terminal gold(I) acetylides¹⁹ (**1**, 1.180(2) and 1.170(2) Å; **2**, 1.177(15) and 1.190(17) Å; **3**, 1.194(12) and 1.199(12) Å; **4**, 1.187(7) and 1.173(7) Å; **5**, 1.186(8) and 1.184(9) Å). The $\text{Au}\cdots\text{Au}$ separations of complexes **1–5** are too long for any $\text{Au}\cdots\text{Au}$ interaction to occur (**1**, 8.567 Å; **2**, 6.696 Å; **3**, 6.729 Å; **4**, 8.764 Å; **5**, 8.870 Å). It is interesting to find that the $\text{Au}\cdots\text{Au}$ distances found in these complexes in the solid state do not follow a trend that is governed by the steric demands of the phosphine ligands alone, in which a $\text{Au}\cdots\text{Au}$ separation of **1** \approx **5** < **2** < **3** < **4** is

expected. Complex **4** with three *p*-tolyl groups attached to each of the phosphorus atoms would be expected to cause the two Au atoms to move further apart in order to avoid the steric hindrance imposed by the neighboring $(\text{R}_n\text{R}'_{3-n}\text{P})\text{Au}$ moieties, while complexes **1** and **5** with no substituents on the phenyl ring and the *o*-tolyl groups on the phosphorus, respectively, would be expected to experience the least steric hindrance between the two $(\text{R}_n\text{R}'_{3-n}\text{P})\text{Au}$ moieties since the methyl substituents on the *o*-tolyl group of $\text{R}_n\text{R}'_{3-n}\text{P}$ in **5** could fold back and direct away from the adjacent $(\text{R}_n\text{R}'_{3-n}\text{P})\text{Au}$ unit. However, in the solid state, different crystal packing forces come into play, giving rise to an unexpected trend. For example, the presence of $\text{C}-\text{H}\cdots\pi(\text{C}\equiv\text{C})$ contacts in the crystal packing of **1**, in which the aromatic protons on

(19) (a) Cross, R. J.; Davidson, M. F. *J. Chem. Soc., Dalton Trans.* **1986**, 411. (b) Yam, V. W. W.; Choi, S. W. K.; Cheung, K. K. *J. Chem. Soc., Dalton Trans.* **1996**, 3411. (c) Yam, V. W. W.; Choi, S. W. K. *J. Chem. Soc., Dalton Trans.* **1996**, 4227.

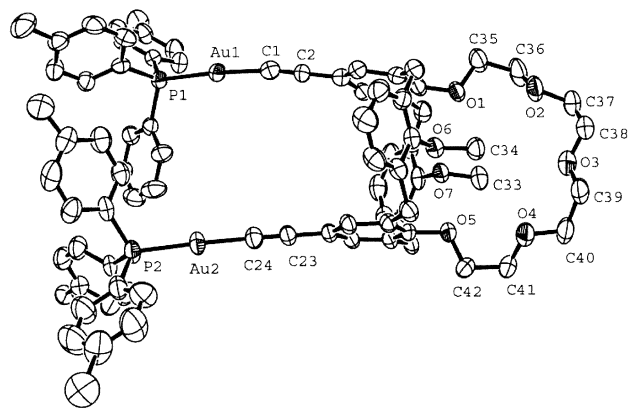


Figure 1. Perspective drawing of complex **3** with atomic numbering. Thermal ellipsoids are shown at the 30% probability level.

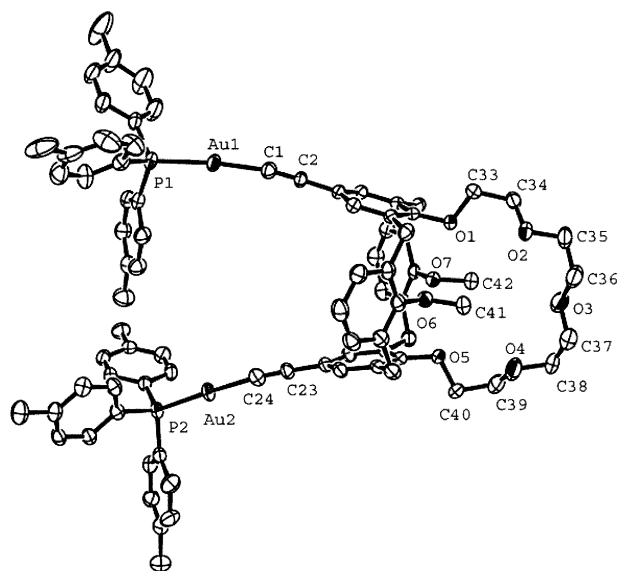


Figure 2. Perspective drawing of complex **4** with atomic numbering. Thermal ellipsoids are shown at the 30% probability level.

the phosphine ligands of one molecule interact with the ethynyl groups on the adjacent molecule, causes the Au...Au distance to be longer than that expected based on steric grounds alone. Similarly, the presence of a C–H... π (C \equiv C) interaction between the hydrogen atom on the dichloromethane solvent molecule and the ethynyl groups in **2** causes the Au...Au distance to be longer than expected. On the other hand, the presence of short Cl... π (C=C) contacts found between the chloro group on dichloromethane and the aromatic rings on the phosphine in **5** causes the Au...Au separation to increase.

Electronic Absorption Spectroscopy. The electronic absorption spectra of complexes **1–5** in dichloromethane solution are mainly dominated by high-energy absorption bands at 270–300 nm and a low-energy band at ca. 342 nm with small extinction coefficients. With reference to previous spectroscopic works on ethynylgold(I) complexes²⁰ and the similarities of the absorption bands with the corresponding free ligands [free ligand absorptions: $\lambda \approx 264$ nm (PPh₃, Ph₂(*p*-Tol)P, Ph(*p*-Tol)₂P, (*p*-Tol)₃P); $\lambda \approx 278$ nm ((*o*-Tol)₃P); $\lambda \approx 268$ –320 nm (ethynylcalixcrown)], the high-energy

Table 2. Selected Bond Distances (Å) and Bond Angles (deg) for **1–5** with Estimated Standard Deviations in Parentheses

[(Ph ₃ P)Au] ₂ L (1)			
Bond Distances (Å)			
Au(1)–P(1)	2.283(3)	Au(2)–C(9)	2.04(1)
Au(2)–P(2)	2.275(3)	C(1)–C(2)	1.18(2)
Au(1)–C(1)	2.04(1)	C(9)–C(10)	1.17(2)
Bond Angles (deg)			
Au(1)–C(1)–C(2)	177(1)	P(1)–Au(1)–C(1)	177.9(4)
Au(2)–C(9)–C(10)	166(1)	P(2)–Au(2)–C(9)	170.5(4)
[Ph ₂ (<i>p</i> -Tol)P]Au] ₂ L (2)			
Bond Distances (Å)			
Au(1)–P(1)	2.282(3)	Au(2)–C(24)	2.028(13)
Au(2)–P(2)	2.288(3)	C(1)–C(2)	1.190(17)
Au(1)–C(1)	1.991(15)	C(23)–C(24)	1.177(15)
Bond Angles (deg)			
C(2)–C(1)–Au(1)	170.5(13)	C(1)–Au(1)–P(1)	176.0(4)
C(23)–C(24)–Au(2)	176.6(11)	C(24)–Au(2)–P(2)	176.6(3)
[Ph(<i>p</i> -Tol) ₂ P]Au] ₂ L (3)			
Bond Distances (Å)			
Au(1)–P(1)	2.282(2)	Au(2)–C(24)	1.998(10)
Au(2)–P(2)	2.283(3)	C(1)–C(2)	1.199(12)
Au(1)–C(1)	2.007(11)	C(23)–C(24)	1.194(12)
Bond Angles (deg)			
C(2)–C(1)–Au(1)	172.4(9)	C(1)–Au(1)–P(1)	174.7(3)
C(23)–C(24)–Au(2)	175.7(10)	C(24)–Au(2)–P(2)	176.6(3)
[(<i>p</i> -Tol) ₃ P]Au] ₂ L (4)			
Bond Distances (Å)			
Au(1)–P(1)	2.2774(16)	Au(2)–C(24)	2.030(6)
Au(2)–P(2)	2.2781(15)	C(1)–C(2)	1.187(7)
Au(1)–C(1)	2.010(6)	C(23)–C(24)	1.173(7)
Bond Angles (deg)			
C(2)–C(1)–Au(1)	171.6(5)	C(1)–Au(1)–P(1)	173.09(16)
C(23)–C(24)–Au(2)	170.7(6)	C(24)–Au(2)–P(2)	176.12(18)
[(<i>o</i> -Tol) ₃ P]Au] ₂ L (5)			
Bond Distances (Å)			
Au(1)–P(1)	2.2879(17)	Au(2)–C(24)	2.010(8)
Au(2)–P(2)	2.2911(18)	C(1)–C(2)	1.186(8)
Au(1)–C(1)	2.004(7)	C(23)–C(24)	1.184(9)
Bond Angles (deg)			
C(2)–C(1)–Au(1)	176.4(7)	C(1)–Au(1)–P(1)	175.8(2)
C(23)–C(24)–Au(2)	177.0(8)	C(24)–Au(2)–P(2)	177.1(3)

absorption bands at ca. 270–300 nm are tentatively assigned as the intraligand (IL) transitions of the phosphine and the ethynylcalixcrown ligand, while the low-energy absorption band at 342 nm, which is not found in the free ligands, may be characteristic of the gold(I) acetylide system.

Emission Properties. All the complexes synthesized show luminescence properties. The solid-state emission spectra of complexes **1–5** all show an emission band at ca. 450–480 nm. The relatively high energy of the emission is suggestive of an origin of metal-perturbed intraligand or σ (Au–P) \rightarrow π^* (R_nR'_{3–n}P) character, in which **5** with the lowest-energy absorbing tri-*o*-tolylphosphine shows the lowest energy metal-perturbed ³IL or σ (Au–P) \rightarrow π^* (R_nR'_{3–n}P) emission in the solid state. The occurrence of the excitation bands at ca. 320 nm, which matches well with the metal-perturbed IL bands in the

(20) (a) Muller, T. E.; Choi, S. W. K.; Mingos, D. M. P.; Murphy, D.; Williams, D. J.; Yam, V. W. W. *J. Organomet. Chem.* **1994**, *484*, 209. (b) Yam, V. W. W.; Choi, S. W. K.; Cheung, K. K. *Organometallics* **1996**, *15*, 1734.

Table 3. Photophysical Spectral Data for 1–5

complex	absorption ^a		emission		
	$\lambda_{\text{abs}}/\text{nm}$ ($\epsilon_{\text{max}}/\text{dm}^3 \text{ mol}^{-1} \text{ cm}^{-1}$)		medium (TK)	$\lambda_{\text{em}}/\text{nm}$ ($\tau_0/\mu\text{s}$)	
1	276 (44440), 286 (48930), 306 sh (31050), 344 (945)		CH ₂ Cl ₂ (298) solid (298) solid (77)	578 (6.7) 465 (1.7) 470	
	2	276 (39850), 286 (43580), 300 sh (32880), 342 (880)		CH ₂ Cl ₂ (298) solid (298) solid (77)	584 (3.7) 476 (5.9) 469
		3	274 (46420), 286 (48910), 300 sh (34820), 342 (740)		CH ₂ Cl ₂ (298) solid (298) solid (77)
4			274 (43410), 286 (46300), 300 sh (29320), 342 (390)		CH ₂ Cl ₂ (298) solid (298) solid (77)
	5		274 (47740), 283 (54720), 298 sh (37480), 341 (365)		CH ₂ Cl ₂ (298) solid (298) solid (77)

^a In dichloromethane at 298 K.

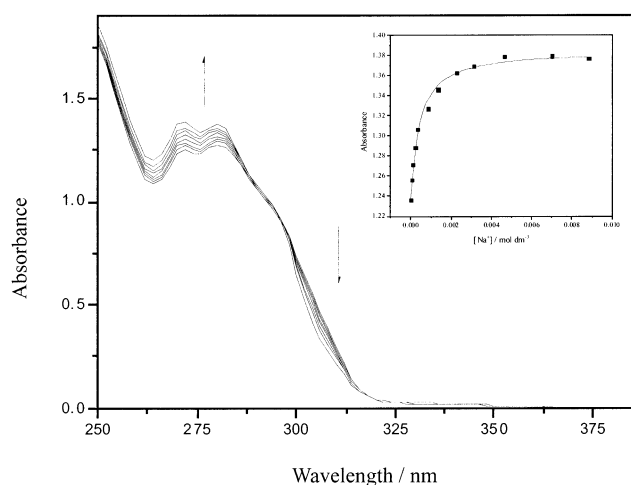


Figure 3. Electronic absorption spectral traces of **4** ($2.5 \times 10^{-5} \text{ mol dm}^{-3}$) in dichloromethane/methanol (1:1 v/v; 0.1 M ⁿBu₄NPF₆) upon addition of NaClO₄. The inset shows a plot of absorbance vs [Na⁺] monitored at $\lambda = 270 \text{ nm}$ (■) and its theoretical fit (—).

electronic absorption spectra, is consistent with such an assignment. The Stokes shifts and the observed lifetimes in the microsecond range for their emissions are suggestive of a triplet parentage.

In dichloromethane, the emission band occurs at ca. 578–585 nm, with excitation bands at ca. 350 nm. The luminescence quantum yields of the complexes are on the order of 10^{-1} , with the luminescence quantum yield of **5** being 0.15. It is likely that the emission is derived from a triplet state of metal-perturbed intraligand or $\sigma(\text{Au}-\text{P}) \rightarrow \pi^*(\text{R}_n\text{R}'_{3-n}\text{P})$ character, typical of the Au(I) phosphine acetylide system.²⁰ The emission of the complexes is found to be sensitive to oxygen quenching, with bimolecular quenching rate constants approaching that of the diffusion-controlled limit.

Cation-Binding Properties. Upon addition of alkali metal cations to a dichloromethane/methanol (1:1 v/v) solution of **1–5**, the intraligand absorption band of alkylnylcalixcrowns exhibits a blue shift in absorption energy. Figure 3 shows the electronic absorption spectral traces upon addition of sodium cations to a solution of **4**, in which a well-defined isosbestic point was observed. The $\log K_s$ values obtained for the binding of

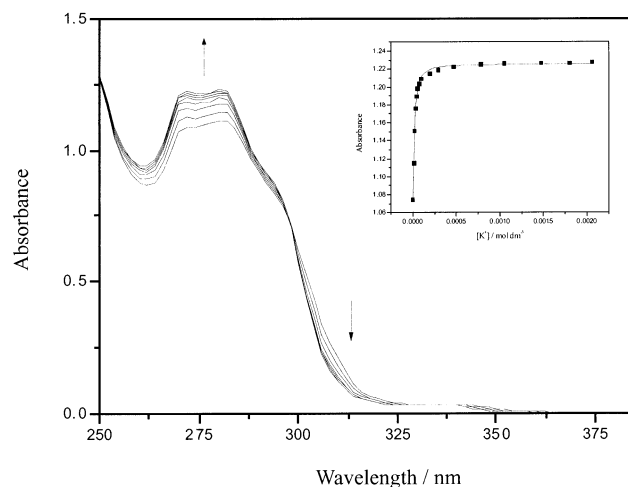


Figure 4. Electronic absorption spectral traces of **2** ($2.5 \times 10^{-5} \text{ mol dm}^{-3}$) in dichloromethane/methanol (1:1 v/v; 0.1 M ⁿBu₄NPF₆) upon addition of KPF₆. The inset shows a plot of absorbance vs [K⁺] monitored at $\lambda = 270 \text{ nm}$ (■) and its theoretical fit (—).

Na⁺ ions are 2.75 ± 0.03 , 2.83 ± 0.02 , 2.38 ± 0.02 , 3.39 ± 0.04 , and 2.97 ± 0.02 for complexes **1–5**, respectively, according to eq 1. A 1:1 complexation stoichiometry was obtained as evidenced by the close agreement of the experimental data to the theoretical fits. In the case of K⁺ ions, the UV–visible absorption spectral traces upon addition of potassium cations to the solution of **2** are shown in Figure 4, in which a well-defined isosbestic point was observed. The $\log K_s$ values for K⁺ ion-binding are 7.24 ± 0.04 , 5.08 ± 0.03 , 4.66 ± 0.03 , and 4.49 ± 0.04 for complexes **1–4**, respectively. Similarly, a 1:1 complexation stoichiometry is evidenced by the close agreement of the experimental data to the theoretical fits. It is interesting to note that the $\log K_s$ for Na⁺ ion-binding follows the order **4** > **5** ≥ **2** > **1** > **3**, while that for K⁺ ion-binding follows the order **5** ≫ **1** > **2** > **3** > **4**. As discussed earlier, on the basis of steric grounds alone and neglecting solid-state effects, complex **4** with three *p*-tolyl groups attached to each of the phosphorus atoms would be expected to give rise to the largest Au...Au separation as a result of the steric hindrance imposed by the neighboring (R_nR'_{3-n}P)Au moieties, and hence a smaller calixcrown cavity size. On the other hand, complexes **1** and **5** would be expected to experience the least steric hindrance between the two (R_nR'_{3-n}P)Au moieties, giving rise to the largest calixcrown cavity. This is in agreement with the observed trends in the ion-binding properties, in which **4** gave the largest binding constant for Na⁺ ion and the least binding constant for K⁺ ion. In fact **5** binds so strongly to K⁺ ion that no satisfactory fit for eq 2 can be obtained. Subtle steric effects of the substituents on the phosphine ligand appear to play an important role in governing the ion-binding properties of the complexes.

The K⁺/Na⁺ selectivities of the complexes **1–4** are 3×10^5 , 1.8×10^2 , 1.9×10^2 , and 13, respectively. As a result, it can be concluded that the dinuclear gold(I) alkylnylcalix[4]crown complexes bind K⁺ ions preferentially over Na⁺ ions. Similar reports on the preferential binding of K⁺ ions over Na⁺ for the cone conformation of the calix[4]crown-5 can be found.²¹

Similar studies using emission methods were unsuccessful since no significant changes in the luminescence properties of the complexes were observed upon addition of metal ions.

Conclusion

A series of dinuclear gold(I) alkynylcalix[4]crown complexes were successfully synthesized and spectroscopically characterized and their structures solved by X-ray crystallography. The electronic absorption and emission behavior of these dinuclear gold(I) alkynylcalix[4]crown complexes have been studied. Binding properties of the complexes toward alkali metal ions have been studied and fine-tuned by a change in the auxiliary ligands. In conclusion, the dinuclear gold(I) alkynylcalix[4]crown complexes have been shown to exhibit interesting electronic absorption and luminescence properties and also shown to function as spectrochemical ion probe. By appropriate design and modification, dinuclear gold(I) alkynylcalix[4]crown complexes have the potential

(21) (a) Ghidini, E.; Ugozzoli, F.; Ungaro, R.; Harkema, S.; Abu El-Fadl, A.; Reinhoudt, D. N. *J. Am. Chem. Soc.* **1990**, *112*, 6979. (b) Ugozzoli, F.; Ori, O.; Casnati, A.; Pochini, A.; Ungaro, R.; Reinhoudt, D. N. *Supramol. Chem.* **1995**, *5*, 179.

to be further developed as selective metalloreceptors for other metal ions.

Acknowledgment. V.W.-W.Y. acknowledges support from The University of Hong Kong Foundation for Educational Development and Research Limited and the University Grants Committee Area of Excellence Scheme. The work described in this paper was supported by the Research Grants Council of the Hong Kong Special Administrative Region, China (Project HKU7097/01P). S.-K.Y. and K.-L.C. acknowledge the receipt of a postgraduate studentship, and N.Z., the receipt of a university postdoctoral fellowship, both administered by The University of Hong Kong.

Supporting Information Available: Perspective drawings of complexes **2** and **5**. Tables giving atomic coordinates, anisotropic thermal parameters, bond lengths, and bond angles for complexes **1–5**. Electronic absorption spectral traces of complexes **2**, **3**, and **5** upon addition of NaClO₄. Electronic absorption spectral traces of complexes **3** and **4** upon addition of KPF₆. The material is available free of charge via the Internet at <http://pubs.acs.org>.

OM030021C